J. Fluid Mech. (1974), *vol.* 64, *part* 4, *pp.* 625–644
Printed in Great Britain

Turbulent/non-turbulent decisions in an intermittent flow

By THOMAS B. HEDLEY† AND JAMES F. KEFFER
Department of Mechanical Engineering, University of Toronto

(Received 28 December 1972)

The purpose of this study is to generalize the experimental method for deciding when a fluid motion can be considered turbulent. The rationale advanced for processing a transducer signal, which indicates the intermittent nature of a turbulent field, is given a probabilistic outlook. In addition an improved detector function is introduced which uses information from longitudinal and lateral fluctuation components.

1. Introduction

The means by which a turbulent medium propagates into a non-turbulent fluid is a particularly interesting and challenging problem. One can easily appreciate the macroscopic features of this process. The large-scale eddies, observable at the free edges of turbulent shear flows, are an obvious mechanism for the lateral growth of the motion and they have been found to play a central role in the entrainment of free-stream fluid (Townsend 1970). At the same time however, any complete explanation must include a description of the small-scale activity: the effective digestion or contamination of the non-turbulent fluid which takes place through the turbulent/non-turbulent interface. There have been only a few attempts at a theoretical explanation of this problem (Phillips 1972; Corrsin & Kistler 1955; Townsend 1970). This is partly a consequence of a lack of detailed knowledge of the physics of the flow at the interface. Such experimental observations are difficult to make accurately since a precise specification of the instantaneous position of the interface is a prerequisite.

Most previous investigations have been concerned with identifying the gross features of the outer motion only and the influence of the turbulent/non-turbulent character upon the flow has been masked. Corrsin (1943) was the first to report detection of these turbulent/non-turbulent patterns, from his examination of the axisymmetric jet. The phenomenon was termed intermittency and the first measurement of the intermittency fraction was made by Townsend (1948), for the turbulent wake generated by a circular cylinder. Assuming that within turbulent zones of the flow the fine-scale structure was homogeneous, Townsend compared the flatness factor of the derivative of the streamwise velocity fluctuations at points throughout the outer regions of the wake with that determined

† Present address: Hatch Associates, Toronto.

on the axis. The ratio of the terms thus gave the intermittency factor directly. Townsend (1949) also introduced a more obvious method using an analog technique which counted periods of time when the turbulent fluctuation quantity (or a variable associated with it) could be judged non-zero. This was followed by the studies by Corrsin & Kistler (1955), who examined the round jet, plane wake and rough-walled boundary layer, essentially using Townsend's methods, and by Klebanoff (1955), who inspected the same variables from film strip records for the boundary layer.

Intermittency measurements have since then been made in a variety of flows using essentially similar methods. The most comprehensive sets of data are those supplied by Kovasznay, Kibens & Blackwelder (1970) for a turbulent boundary layer and Wygnanski & Fiedler (1970) for a mixing layer. Both groups extended the techniques to allow zonal and point averages of the variables to be made and were thus able to identify characteristics of purely turbulent and non-turbulent fluid in the intermittent region. The replacement of the complicated electronic treatment of the signals by digital sampling techniques would appear to be a desirable step but it is only fairly recently that this approach has become feasible (Kaplan & Laufer 1968; Antonia & Bradshaw 1971).

In principle the essential features of the problem of deciding when a flow can be judged turbulent are easily defined but they involve arbitrary and subjective decisions. In previous work the rationale behind these various decisions has often not been clear. Our present investigation attempts to explore these questions in some detail. On-line digital sampling techniques for the acquisition and processing of the data have been used exclusively because of the flexibility and power which they afford although the physical interpretation applies equally well to analog treatments.

2. The intermittent motion

The statistics of the conditional sampling and averaging of an intermittent signal are described by Kovasznay *et al.* (1970). We review here briefly some details which are appropriate to our present digital techniques.

The flow variables in turbulent motion are statistically random quantities. To discuss their behaviour in an intermittent region of the flow it is convenient to assume that they come from two mutually exclusive populations associated with the non-turbulent and turbulent fluid. We consider a typical flow variable $Q(r,t)$, which can represent quantities as widely different as a velocity component or the width of a turbulent burst. The continuous measurement of $Q(r,t)$ during an experiment can be considered as one realization from an infinite ensemble. To ensure that averages taken over a realization are equivalent to averages over the entire ensemble it is necessary that all possible scales of variability be present within the sample. This simply means that the record must be long enough to include the largest integral scales (Lumley & Panofsky 1964). When this is true the experimental realization can be regarded as a sequence of individual experiments, each at least two integral scales in length and each independent of the others (Sheih, Tennekes & Lumley 1971). The equivalence of an average

taken over these experiments to the true ensemble average is the ergodic hypothesis usually adopted.

In the evaluation of temporal averages only a single experimental realization need be considered. The overall ensemble average is thus

$$\bar{Q}(r) = \sum_{i=1}^{N} \frac{Q(r,t_i)}{N},$$

where N is taken large enough to satisfy some stability criterion. If we now introduce the indicator function I of Kovasznay *et al.* to identify the turbulence, so that it is unity within the turbulent fluid and zero otherwise, the expected value of I is

$$\bar{I}(r) = \sum_{i=1}^{N} \frac{I(r,t_i)}{N}.$$

This is the turbulent fraction or 'intermittency factor'.

When evaluating expected values in turbulent and non-turbulent zones, one carries out the appropriate conditional averaging as follows. (We have adopted the overbar symbolism of Kovasznay *et al.* for these averages.) In the turbulent fluid,

$$\overline{\tilde{Q}}(r) = \sum_{i=1}^{N} \frac{I(r,t_i)\,Q(r,t_i)}{N\bar{I}(r)}$$

and in the non-turbulent zones,

$$\widetilde{\tilde{Q}}(r) = \sum_{i=1}^{N} \frac{[1-I(r,t_i)]\,Q(r,t_i)}{N[1-\bar{I}(r)]}.$$

The constraint on these zone averages is simply

$$\bar{Q}(r) = \bar{I}(r)\,\overline{\tilde{Q}}(r) + [1-\bar{I}(r)]\,\widetilde{\tilde{Q}}(r).$$

Conditional average values at specific locations with respect to the position of the turbulent/non-turbulent interface can also be defined. Such ensemble means are designated $\hat{Q}(r)$ and are called point averages.

With the introduction of zonal and point averages, it becomes necessary to place some constraints upon the many possible definitions of the fluctuation intensities. For example, if

$$q(r,t) = Q(r,t) - \bar{Q}(r), \quad q_t(r,t) = Q(r,t) - \overline{\tilde{Q}}(r),$$

$$q_n(r,t) = Q(r,t) - \widetilde{\tilde{Q}}(r), \quad q_p(r,t) = Q(r,t) - \hat{Q}(r),$$

then the only physically meaningful intensities are those evaluated in the corre sponding domains, i.e.

$$\overline{q^2}(r), \quad \overline{\tilde{q}_t^2}(r), \quad \widetilde{\tilde{q}_n^2}(r), \quad \hat{q}_p^2(r) \quad (\text{or } \langle [Q(r,t) - \hat{Q}(r)]^2 \rangle).$$

We note that the simple temporal average of say $q_t(r,t)$ is generally non-zero,

$$\bar{q}_t(r) = \bar{Q}(r) - \overline{\tilde{Q}}(r) \neq 0,$$

while the zonal average, by definition, must be

$$\overline{\tilde{q}_t}(r) = \bar{\tilde{Q}}(r) - \bar{\tilde{Q}}(r) = 0.$$

The relationship between the mean-square intensity fluctuations is given by

$$\overline{q^2}(r) = \bar{I}\overline{\tilde{q}_t^2}(r) + (1-\bar{I})\,\overline{\tilde{q}_n^2}(r) + \bar{I}(1-\bar{I})\,[\tilde{\bar{Q}}(r) - \bar{\tilde{Q}}(r)]^2.$$

3. Turbulent/non-turbulent decisions

3.1. *The processing of the signal*

Two distinctive features of the turbulent fluid are its three-dimensional rotational nature and the dissipation of mechanical energy into heat through a cascade of eddies of diminishing size. The detection of an energy cascade requires a spectral analysis and it is difficult to use this in an instantaneous decision for or against the presence of turbulence. Rather, vortical fluctuations, which are characteristic of the instantaneous local angular momentum, are a more appropriate choice for discrimination. Unfortunately the detection of this signal requires a complex probe capable of spatial differentiation. The technique has been used by Corrsin & Kistler (1955), and most recently by Kibens & Oswald (1974). However, the operational difficulties appear to outweigh the advantages for most experimentalists. As well, the spatial resolution of such a probe can be inherently large and this limits the precision with which the interface may be specified.

Alternatively it is possible to identify the fine-scale structure of the flow independently, using a simpler signal such as the velocity fluctuation. A disadvantage is that such a variable is not unique to the turbulent fluid and we must sensitize it in some manner to increase its discriminatory capability. The method most commonly used is to differentiate or high-pass filter the signal and square it thus emphasizing the high frequency components. At this point two arbitrary decisions are made. There will be some periods of time when the processed signal or detector function will have zeros within fully turbulent fluid since its amplitude probability density function is continuous down to the origin, although everywhere positive. Such 'legitimate zeros' will influence any decision for or against the presence of turbulence. The conventional method of eliminating this effect is to smooth or short-term integrate the signal over a small period of time T_s, which produces a criterion function $S(r,t)$. Next it is necessary to establish a threshold level C for this criterion function, to discriminate between the true turbulence and signal 'noise' which will inevitably exist regardless of the choice of detector function. Applying the threshold level then produces an indicator function satisfying

$$I(r,t) = \begin{cases} 1 & \text{when} \quad S(r,t) \geqslant C, \\ 0 & \text{when} \quad S(r,t) < C. \end{cases}$$

This random square wave is then carried along with the original signal and used to condition the appropriate averages. The procedure is shown schematically

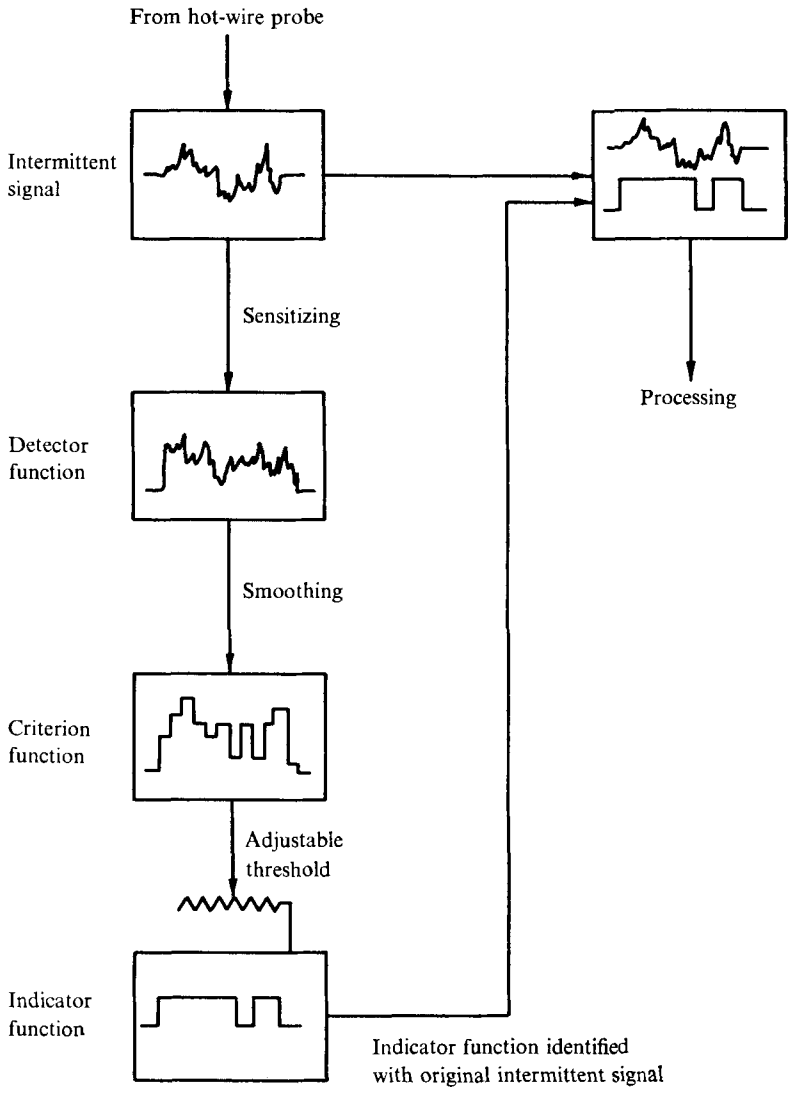

FIGURE 1. Schematic diagram of the generation of the indicator function.

in figure 1 and the implications of these decisions are discussed in the following sections.

3.2. *The detector function*

We choose to examine the above operations by discussing the signal processing in terms of the effect upon the basic probability density functions of the detector variable. Examples of such variables which have been used previously are given in table 1. For simplicity, we restrict the discussion now to a single fluctuation component q, which could be, for example, the streamwise velocity. Probability density functions of this variable have in fact been measured within fully turbulent fluid by a number of workers (Kuo & Corrsin 1971; Townsend 1948;

Townsend (1949)	$\lvert u\rvert$, $\lvert \partial u/\partial t\rvert$
Corrsin & Kistler (1955)	$\lvert u\rvert$, $\lvert \partial u/\partial t\rvert$
Heskestad (1965)	u^2
Gartshore (1966)	$\lvert \partial u/\partial t\rvert$
Fiedler & Head (1966)	$\lvert \partial u/\partial t\rvert$
Kaplan & Laufer (1968)	$(\partial u/\partial t - \langle \partial u/\partial t\rangle)^2$
Wygnanski & Fiedler (1970)	$(\partial u/\partial t)^2 + (\partial^2 u/\partial t^2)^2$
Kovasznay *et al.* (1970)	$\lvert \partial^2 u/\partial y\, \partial t\rvert$
Antonia & Bradshaw (1971)	$(\partial u/\partial t)^2$
Sunyach (1971)	$(\partial u/\partial t)^2$ filtered
Antonia (1972)	$(\partial uv/\partial t)^2$
Thomas (1973)	$\lvert \partial u/\partial t\rvert$ filtered
Bradshaw & Murlis (1973)	$\lvert \partial uv/\partial t\rvert$ or $\lvert \partial^2 uv/\partial t^2\rvert$

TABLE 1. Turbulence detector functions

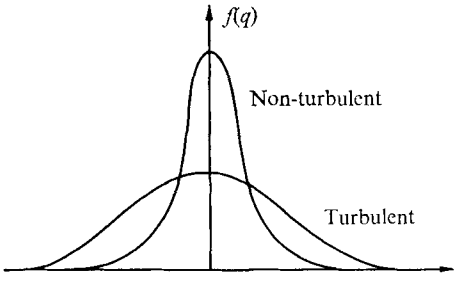

FIGURE 2. Hypothetical probability density function for the turbulent and non-turbulent fluid.

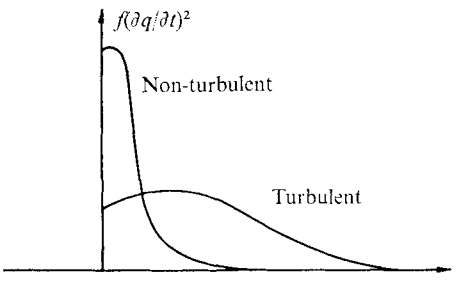

FIGURE 3. The effect of sensitizing on the probability density function.

Van Atta & Chen 1970; Sheih *et al.* 1971). Their results show that the variable itself tends to be distributed normally about zero but deviations from this normal shape increase progressively with the order of the derivative.

In the intermittent fluid, we assume q to have a random distribution of amplitude in both the turbulent and non-turbulent domains. The corresponding normalized probability density functions are shown qualitatively in figure 2. (We ignore here the differences in mean convective flow within the turbulent and non-turbulent regions.) This representation is physically acceptable. Within the non-turbulent zones, fluctuations in q are of small amplitude whereas within the turbulent fluid, a broader distribution of amplitude variation is expected. This behaviour is confirmed directly by the recent results of Thomas (1973) for a two-dimensional turbulent wake. His data show, however, a marked skewness in the turbulent zone probability density function, a detail we may ignore for purposes of the present discussion.

The aim of sensitizing q is to accentuate the differences in shape of the corresponding distributions. For example, if we applied a simultaneous differentiation and squaring of q, the effect would be as is shown in figure 3. In the non-turbulent fluid, the probability of $(\partial q/\partial t)^2$ taking a magnitude significantly larger than

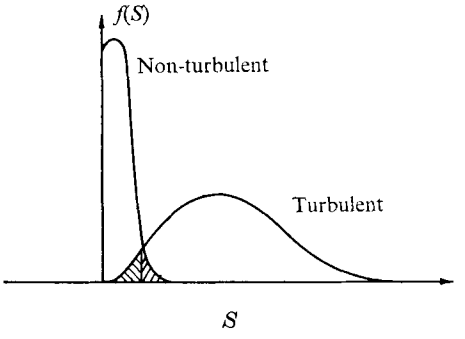

FIGURE 4. Criterion function produced by smoothing.

zero has been reduced relative to that within the turbulent region. We note, however, that the probability of $(\partial q/\partial t)^2$ having small amplitude fluctuations in the turbulent fluid remains non-zero.

3.3. *The smoothing period*

The existence of a large portion of the turbulent probability density function in the region close to the origin imposes a fundamental difficulty in making the decision for or against turbulence. Ideally we would wish to separate the density functions along the horizontal axis and so reduce the overlap. The operation of smoothing the signal achieves this and gives the result shown approximately in figure 4. The remaining overlap of the distributions, now relatively small, represents the probability of making an incorrect statistical choice.

Bradshaw & Murlis (1973) point out that the distribution of turbulent burst lengths is continuous down to the finest scales of the motion and the imposition of an arbitrary hold time must effectively truncate the detection procedure. The choice of smoothing period can be based, however, on physical reasoning. If we accept a margin or error of the order of the smallest eddies for identifying the turbulent burst (certainly a reasonable lower limit), the optimum hold time will be of the order of the Kolmogorov length scale divided by the convection velocity of the smallest eddies (Townsend 1966; Antonia 1972). We note, however, that the practical smoothing period is often considerably greater since it is influenced by the resolution of the probe and the sampling time.

A related problem compounds the difficulty. It is known that, at high enough Reynolds numbers, a degree of spatial localization of the fine-scale turbulent structure occurs (Oboukov 1962; Kuo & Corrsin 1971), producing a form of spectral intermittency. Results indicate that the domains of this fine structure are much larger than the scales of the fine structure itself. The dimensions are 15–35 times the Kolmogorov length. When using higher-order derivatives as a criterion to test for turbulence we weight the fine-scale features of the flow and one may in fact be testing for spectral rather than interfacial intermittency. It may thus be argued that the practical smoothing period should be no smaller than these spectral domains. This is discussed more fully by Bradshaw & Murlis (1973).

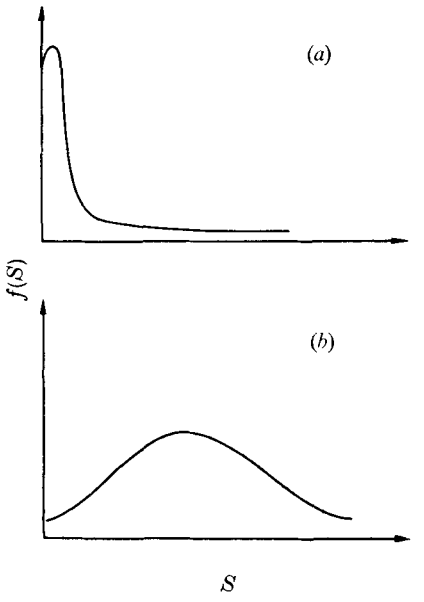

FIGURE 5. Typical probability density function for (a) $P(\tau)$ small and (b) $P(\tau)$ large.

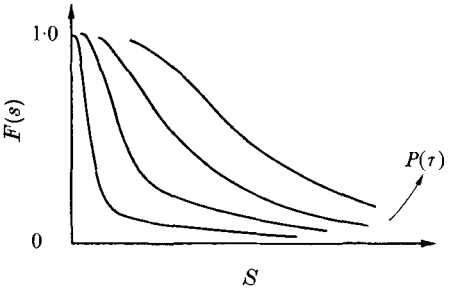

FIGURE 6. Cumulative distribution functions with parametric variation of $P(\tau)$.

3.4. *The threshold level*

An acceptable choice of the threshold level C could be taken as the value of S which equalizes the probabilities of making an incorrect statistical decision in the probability density functions for the two regions. This point is shown by the shaded areas in figure 4. Unfortunately, the distributions are available only *a posteriori*. The overall density function can be obtained however, and this will be the sum of $f_t(S)$ and $f_n(S)$ weighted by the appropriate probability:

$$f(S) = f_t(S)\,P(\tau) + f_n(S)\,[1 - P(\tau)],$$

where $P(\tau)$ is the probability of occurrence of turbulence. With low $P(\tau)$ the distribution will have the form given in figure 5(a). At high levels, the function will take the shape shown in figure 5(b). Because it is experimentally easier to determine the integral or cumulative distribution function, we evaluated

$$F(S) = \int_S^\infty f(\phi)\,d\phi$$

with the limits chosen so that $F(S)$ approaches zero as S approaches infinity. A qualitative illustration of $F(S)$ with $P(\tau)$ as a parameter is shown in figure 6.

The above distribution function has been used by Corrsin & Kistler (1955), Heskestad (1965), Fiedler & Head (1966) and others for their detector variables in deciding upon threshold levels. Generally, the region of maximum curvature was used as a criterion. This point is well defined at low values of $P(\tau)$ but with high levels of turbulence the choice of threshold level becomes highly questionable. Kaplan & Laufer (1968) and Antonia & Bradshaw (1971), with digital methods,

used somewhat similar techniques. In the former, an arbitrary fraction of the local maximum of the criterion function was employed while Antonia & Bradshaw took a fraction of the average of the function over the entire record as their level. In both instances, the level actually used was influenced by a visual comparison between the indicator function and the original signal.

3.5. *The distribution of turbulent fluid*

The contortions of the turbulent front convecting past the probe produce on/off periods of turbulence T_t and non-turbulence T_n. The ensemble-averaged values $\langle T_t \rangle$ and $\langle T_n \rangle$ are in effect large eddy time scales for the motion. At a particular threshold setting the distribution function is in these terms

$$F(C) = \langle T_t \rangle / [\langle T_t \rangle + \langle T_n \rangle]$$

and depends only upon the relative proportion of turbulent fluid. Clearly, $F(C)$ by itself cannot be a sensitive indicator of the structure of the flow since this fraction can arise in an infinity of ways. Of more interest is the frequency $f_\wedge$ of occurrence of these zones, which is defined as the number of positive (or negative) changes in the indicator function I, per second. Thus

$$f_\wedge = [\langle T_t \rangle + \langle T_n \rangle]^{-1}.$$

This variable is particularly sensitive to small changes in both smoothing time and threshold level. For this reason we examine the ensemble-averaged periods of the turbulent and non-turbulent zones as a basis for choosing the threshold level. These are

$$\langle T_t \rangle = F(C)/f_\wedge, \quad \langle T_n \rangle = [1 - F(C)]/f_\wedge,$$

which incorporate information on the average number of zones and the relative size $F(C)$ of the total time periods.

As an integral function, $F(S)$ must naturally decrease monotonically with increasing threshold level. The behaviour of $f_\wedge$ is more difficult to predict however. Antonia & Bradshaw found that $f_\wedge$ remained relatively unaffected by the threshold level over their operating range of S values. As they pointed out, this implies that (with repeated scanning of the same record) the total number of turbulent bulges remained unchanged. It is probable that the total fraction of turbulent fluid continued to change since the widths of the bursts would decrease. In contrast, our results show a marked variation of $f_\wedge$ with the threshold level (see §5.3). Stability with respect to adjusting C was achieved only when we examined the average non-turbulent time period $\langle T_n \rangle$.

4. Experimental considerations

Experiments were performed on a flat-plate turbulent boundary layer in a stream with an approximately zero pressure gradient. The characteristics of the flow, details of the experimental facilities and the techniques for digital data acquisition and processing of the signals are described fully in the companion paper (Hedley & Keffer 1974).

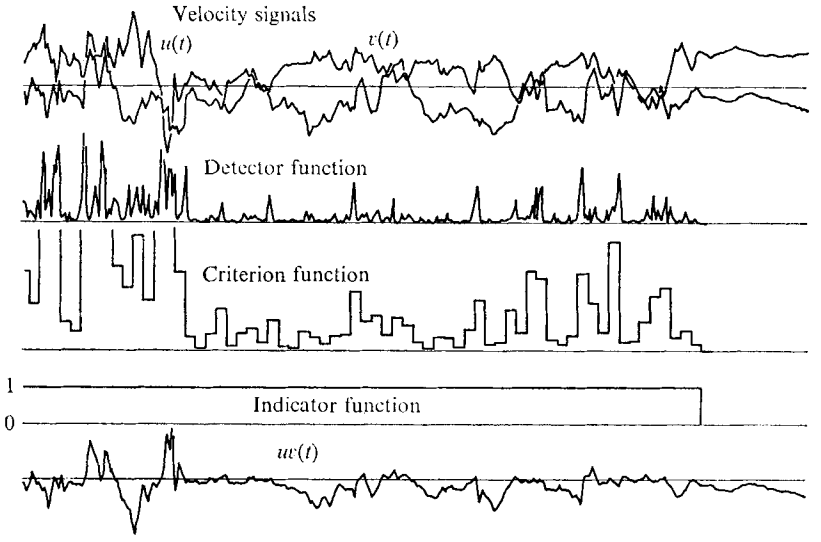

FIGURE 7. Typical computer plots of the turbulence variables for $\bar{I} = 0{\cdot}86$, $y/\delta = 0{\cdot}48$. $u(t) = U - \langle U \rangle$.

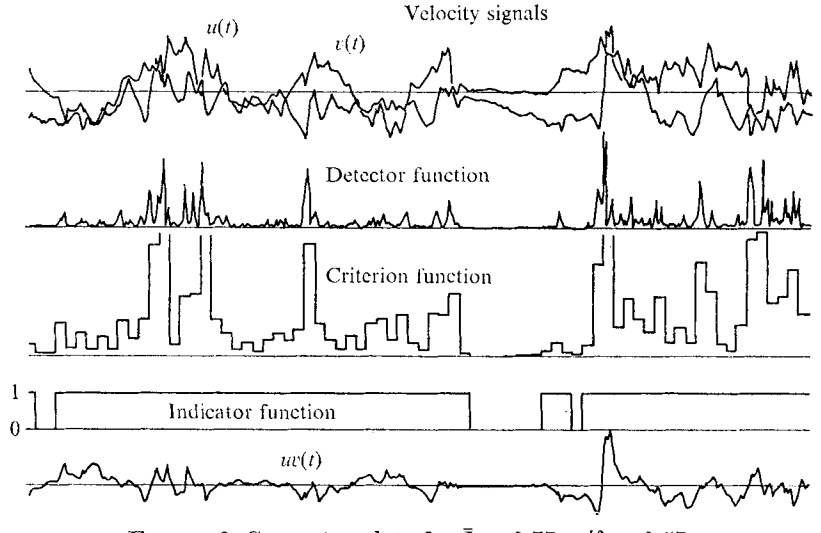

FIGURE 8. Computer plots for $\bar{I} = 0{\cdot}77$, $y/\delta = 0{\cdot}57$.

Generally, when output signals from the transducers are digitized directly and processed by computer, a certain perspective is lost. As a check on the procedure, sample print-outs of the pseudo-analog signal were constructed from the digitized data periodically. These did not contribute in a quantitative way to the analysis but functioned similarly to the monitoring of the experiment by an oscilloscope. Some typical results for various positions through the depth of the boundary layer are shown in figures 7–11. In each, the various stages of the sensitizing, smoothing and application of the threshold level can be traced. The

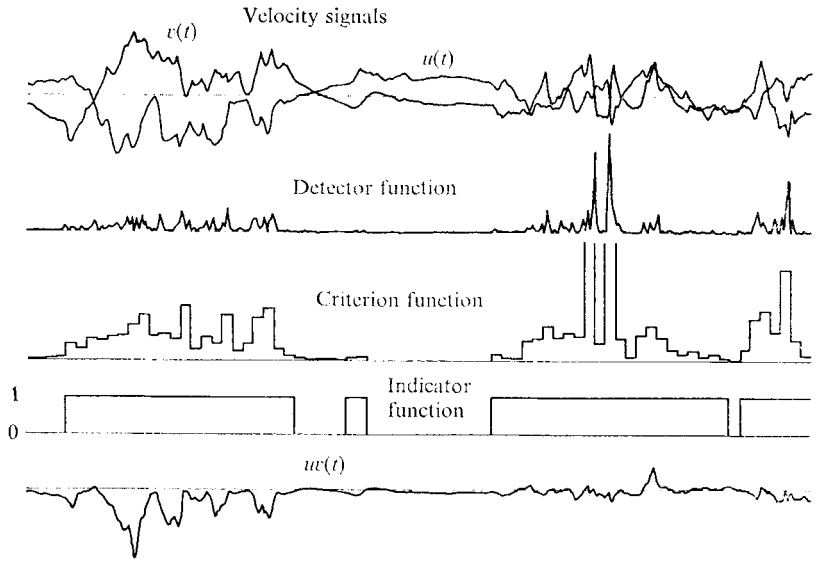

FIGURE 9. Computer plots for $\bar{I} = 0{\cdot}63$, $y/\delta = 0{\cdot}66$.

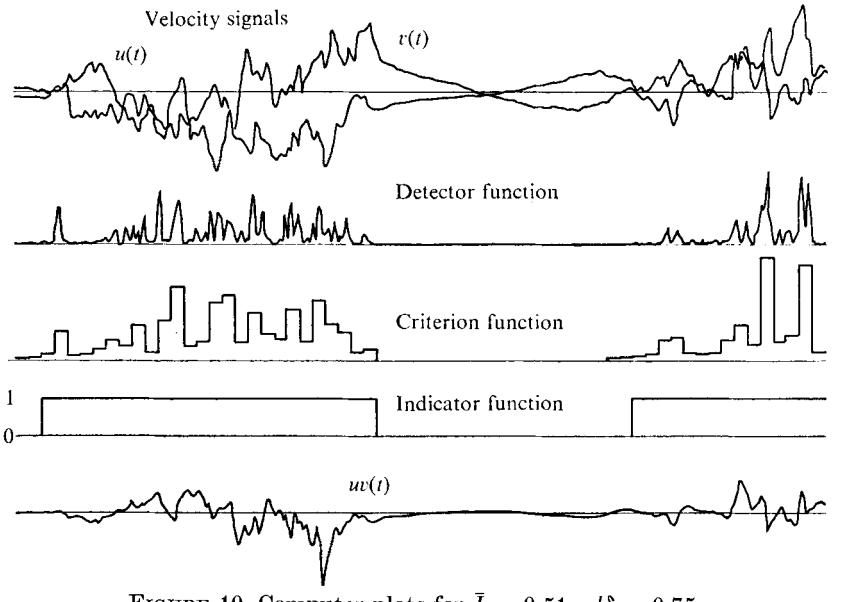

FIGURE 10. Computer plots for $\bar{I} = 0{\cdot}51$, $y/\delta = 0{\cdot}75$.

sampling rate was 10^{-4} s and the portion of record shown in each figure represents approximately 0·03 s.

5. Experimental results

5.1. *The choice of a detector function*

Because the turbulent field is inherently three-dimensional, it is possible, if using only a single fluctuating component, to miss some aspects of the motion.

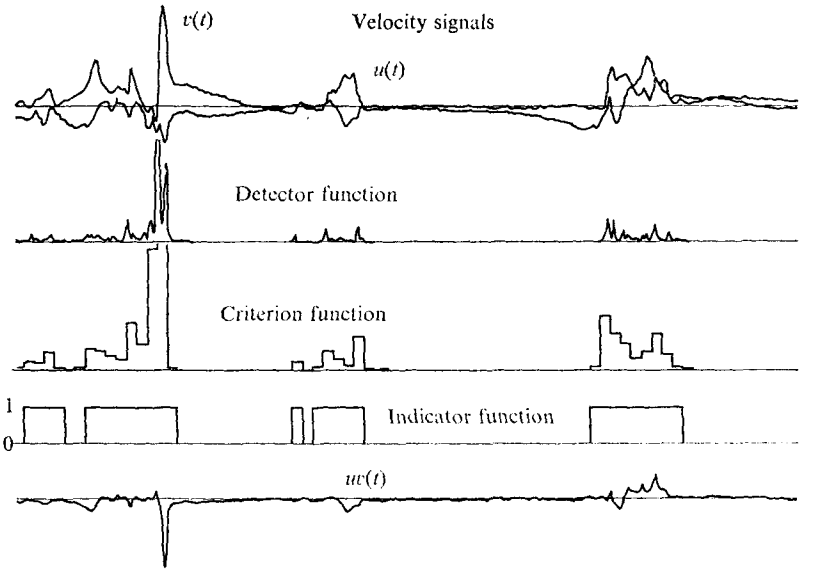

FIGURE 11. Computer plots for $\bar{I} = 0{\cdot}23$, $y/\delta = 0{\cdot}93$.

For this reason it is necessary to choose a basic detector function which incorporates information from both U and V signals at least. An obvious possibility is the instantaneous Reynolds stress and/or one or more of its derivatives. However, our results indicate (Hedley & Keffer 1974) that at the leading edges of the turbulent zones the Reynolds stress exhibits a lack of definition. One would expect of course that the process of sensitizing the signal would improve the discrimination. We chose instead a double-component function which involved the derivatives of U and V separately. In finite-difference form this was

$$[(\Delta u/\Delta T)^2 + (\Delta v/\Delta T)^2].$$

To increase the definition of point averages, a second criterion function

$$[(\Delta^2 u/\Delta T^2)^2 + (\Delta^2 v/\Delta T^2)^2],$$

the derivative of the above, was applied simultaneously, with only a slight increase in computer time.

5.2. *Smoothing periods*

The characteristic times for the various small-scale quantities are listed in table 2. An obvious constraint on the hold time is that T_s could not be less than the maximum digital sampling rate, in our case 10^{-4} s. As an initial estimate we used the Taylor microscale

$$\lambda = \left\{\frac{\langle u^2 \rangle}{\Delta^2 u/\Delta T^2}\right\}^{\frac{1}{2}} \bar{U}.$$

It is pointed out by Bradshaw & Murlis (1973), however, that this is not a suitable quantity for examining the smallest scales of the motion. Rather some multiple of the Kolmogorov length is more meaningful. For high enough Reynolds numbers

Convection time across the probe	$< 0{\cdot}0001$ s
Sampling time interval, ΔT	$= 0{\cdot}0001$ s
Peak of the u spectrum	$\sim 0{\cdot}002$ s
Characteristic time, T_{ch}	$< 0{\cdot}0001$ s
Microscale time, λ/U	$\sim 0{\cdot}0005$ s
Kolmogorov time, $l_k/\bar{U}$	$\sim 0{\cdot}00001$ s
Smoothing time, T_s	$= 0{\cdot}0004$ s

TABLE 2. Smoothing scales

	$\langle L_t \rangle/\delta$	L_s/δ	$\langle L_t \rangle/L_s$
Corrsin & Kistler	1·28	0·254	5·05
Kaplan & Laufer	—	0·393	—
Kovasznay *et al.*	0·67	0·213	3·14
Antonia & Bradshaw	0·35	0·044	8·00
Present study	0·46	0·035	10·54

TABLE 3. Turbulence indicator function resolution ($\bar{I} = 0{\cdot}5$)

we can assume the flow to be locally isotropic, so that λ is related to the Kolmogorov scale l_k by

$$\lambda/l_k = 15^{\frac{1}{4}} Re_\lambda^{\frac{1}{2}},$$

where Re_λ is the Reynolds number based on the microscale.

In this study λ/l_k was approximately 36 while $\lambda/(\bar{U}\Delta T)$ (for $\Delta T = 10^{-4}$ s) was about 5. Kuo & Corrsin (1971) suggest that the flow field should be viewed through a window with dimensions of the order of 15 to $35 l_k$. Additionally, for reasons of symmetry, it is necessary to weight past and future input to the smoothing equally, which merely requires that we use an even number of ΔT intervals. This is essentially a central-difference time-derivative procedure. Within these constraints the smoothing window size L_s and smoothing time T_s were chosen as

$$L_s/\bar{U}\Delta T = T_s/\Delta T = 4.$$

In terms of the Taylor microscale, $L_s/\lambda = \frac{4}{5}$, whereas in terms of the Kolmogorov length, $L_s/l_k = 28$, an order of magnitude greater.

The above choice is a compromise since we now reject all turbulent zones having a duration shorter than about the length of the microscale. Coincidently, the details of the interface are obscured at levels, say, of the Kolmogorov scale. We note from table 3 that the level of resolution based on the nominal depth of the flow is slightly better than in previous work and the present choice can be considered satisfactory.

When the smoothing period is applied to the detector variables, the resulting criterion functions are

$$S(r, t_j) = \frac{\Delta T^2}{1 + T_s/\Delta T} \sum_{i=j-T_s/2\Delta T}^{i=j+T/2\Delta T} \left\{ \left(\frac{\Delta u}{\Delta T}\right)^2 + \left(\frac{\Delta v}{\Delta T}\right)^2 \right\}_i,$$

$$S_0(r, t_j) = \frac{\Delta T^4}{1 + T_s/\Delta T} \sum_{i=j-T/2\Delta T}^{i=j+T/2\Delta T} \left\{ \left(\frac{\Delta^2 u}{\Delta T^2}\right)^2 + \left(\frac{\Delta^2 v}{\Delta T^2}\right)^2 \right\}_i.$$

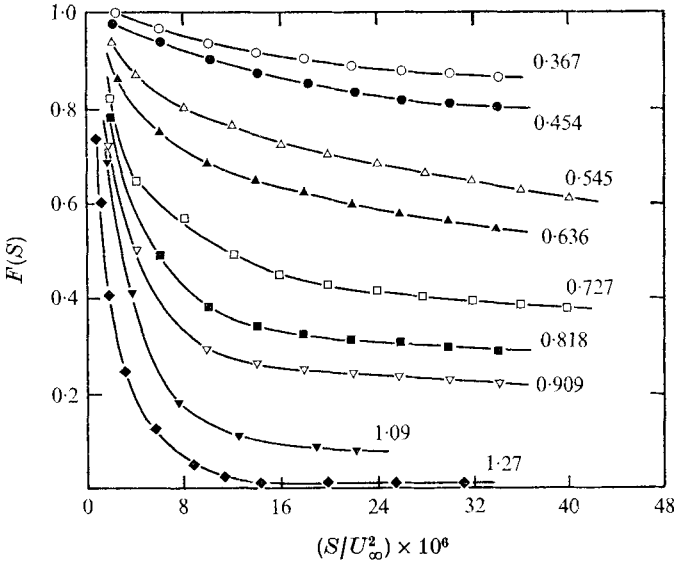

FIGURE 12. Cumulative distribution functions for various y/δ.

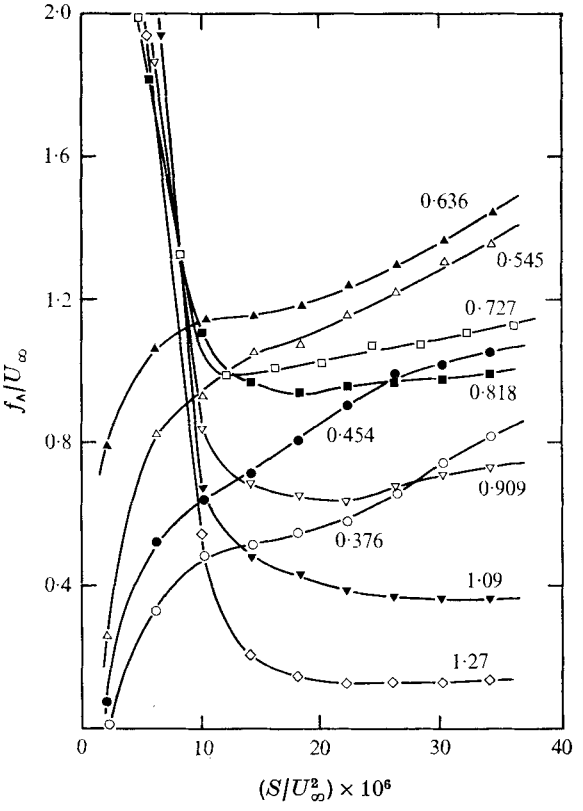

FIGURE 13. Non-dimensional crossing frequency at various y/δ.

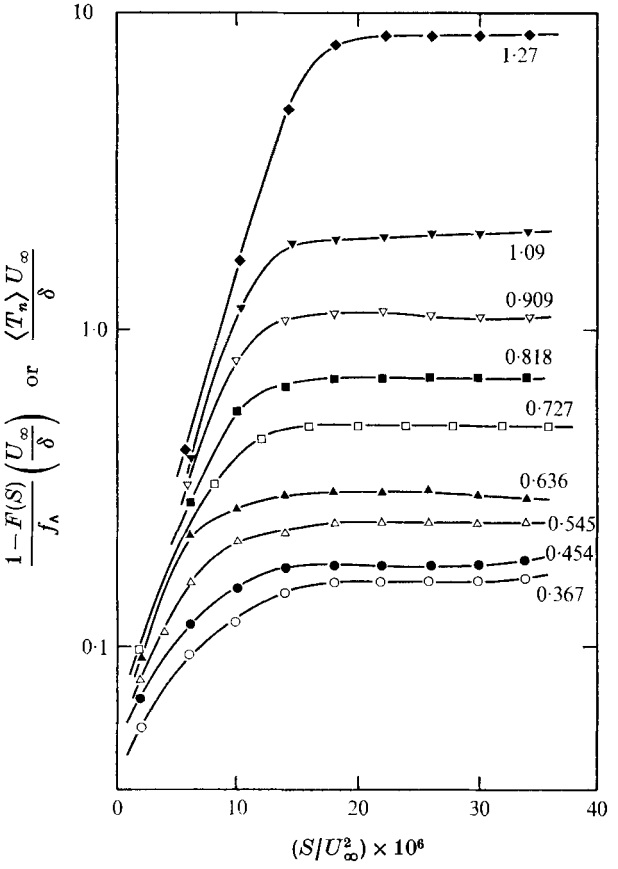

FIGURE 14. Influence of threshold setting for various y/δ.

5.3. *Threshold level*

The difficulties in choosing an appropriate setting for the threshold level C have been outlined above. An attempt was first made to use the simple cumulative distribution function of S. The set of distribution functions for various positions within the boundary layer were evaluated with the results shown in figure 12. We have plotted S non-dimensionalized with respect to the constant free-stream velocity rather than as a fraction of an average of S since we wished to examine absolute changes with respect to y/δ. The results are similar to those found by Corrsin & Kistler (1955) and others. Although there is a monotonic decrease in $F(S)$ with increasing S, a universal sharp break in the slope does not exist for all positions within the boundary layer. Close to the wall where the proportion of turbulence is high it is not obvious what an acceptable value of C should be and this simple approach was thus discarded.

The average crossing frequency f_Λ was next extracted and is plotted non-dimensionally in figure 13. The physical interpretation of these results is interesting. In the outer intermittent regions, the raw signal has many low amplitude, fine-scale features. We can assume this to be noise and it is eliminated by

an increase in the threshold level. In contrast, in the less intermittent region where the proportion of non-turbulent fluid is reduced, increasing C identifies a larger number of turbulent bursts as we begin to encounter the structure superimposed on the relatively high background level of intensity. Again, distinctive changes in the slope of $f_\wedge$ do not exist for all y/δ, which precludes this being used as a sole criterion to establish C.

The evaluation of the distribution function of $\langle T_n \rangle$, the non-turbulent zone width, was carried out next with the result shown in figure 14. It is seen that, regardless of y/δ, the functions increase rapidly, then reach a plateau. Clearly, a continued increase in S must cause $\langle T_n \rangle$ to rise again as the low intensity bulges are eliminated. This was confirmed for a few of the positions but has not been included in the general results. We infer from this that the average distance between the turbulent bursts has stabilized over a significantly large range of threshold levels to enable a simple choice of C. It is not an absolute criterion for the turbulence but the existance of a marked plateau with identical break-points in the curves for all positions across the boundary layer is encouraging and presents a physically acceptable situation for the definition.

The proper non-dimensionalization of these results poses some difficulties, however. For example, Antonia (1972) uses the instantaneous value of $(\partial uv/\partial t)^2$ as his criterion function and takes 0·3 of the overall mean value of this quantity as the threshold level. This procedure can be criticized since the overall mean is a weighted value and it varies markedly throughout the depth of the flow. Alternatively, Bradshaw & Murlis (1973) suggest expressing C in terms of a variable defined within the turbulent zone only. This is certainly an improvement but results indicate that even these quantities may be expected to change with position in the flow. If it is possible to regard turbulence (or non-turbulence) as an absolute state of the fluid in a given flow field, then it follows that a suitably chosen threshold level should also be constant everywhere in that flow. An absolute specification of C would thus be appropriate. If, however, the existence of turbulence is definable only in relative terms, i.e. with respect to a local average level of intensity say, it would be necessary to choose a representation similar to that of Bradshaw & Murlis. To avoid these questions we have chosen to leave the data in absolute terms for the present.

An appropriate evaluation of the threshold level should actually be made for each of the criterion functions S and S_0. But it is not unreasonable that turbulent-fluid time scales would change very little across the outer boundary-layer regions and as an approximation, which *a posteriori* was found to be valid, the ratio $\langle S \rangle / \langle S_0 \rangle$ was measured in the fully turbulent fluid and used as a characteristic time scale T_{ch}. The threshold level for the second criterion function C_0 was thus taken to be C/T_{ch}^2, so that

$$I = \begin{cases} 1 & \text{if } S > C \text{ and/or } S_0 > C_0, \\ 0 & \text{if } S < C \text{ and/or } S_0 < C_0. \end{cases}$$

Inspection of figures 7–11 shows a good correspondence between periods of rapid velocity fluctuation (i.e. turbulence) and proportions of time when the

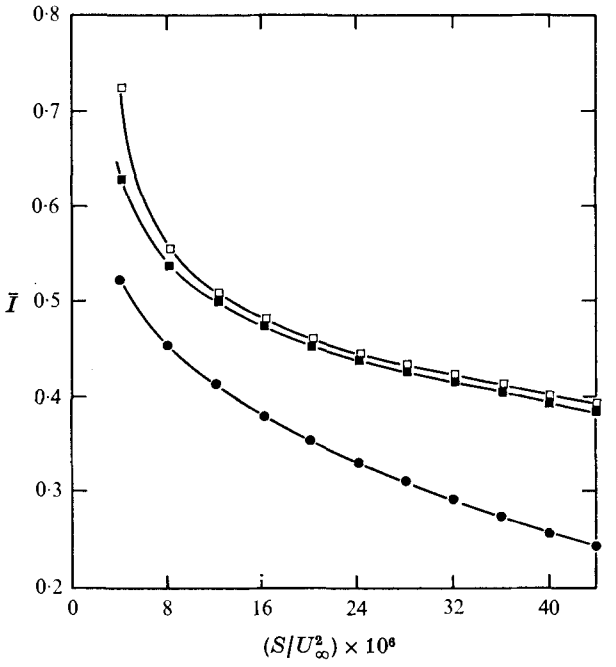

FIGURE 15. Evaluation of cumulative distribution function using various detector functions. □, S and S_0; ●, S; ■, $(\partial u/\partial t)^2$.

indicator function $I = 1$. Furthermore, the agreement was obtained without any visual feedback, that is to say, without adjustment of the threshold level on the basis of subjective matching of previously determined traces.

In an attempt to assess the quality of our technique we explored the effect of altering the basic detector function. Our results showed that, using only the streamwise component $\partial u/\partial t$ of the fluctuating velocity the zones of turbulence detected would be significantly reduced, i.e. the distribution of the intermittency factor $\bar{I}$ would shift towards the wall. This can be seen in figure 15. As well, the crossing frequency f_Λ was found to increase markedly; see figure 16. The effect of using S and S_0 rather than S alone appears rather marginal. As expected, the crossing frequency shows the largest effect. From visual inspection of the traces we concluded that the interface was more precisely defined by including the second derivative and so S_0 was used for all investigations. Ratios of the conditionally averaged criterion functions, which demonstrate the signal separation or 'noise level', are shown in figure 17. Both $\tilde{\tilde{S}}/\tilde{\tilde{S}}$ and $\tilde{\tilde{S}}_0/\tilde{\tilde{S}}_0$ are greater than 50 over most of the intermittent region. This compares favourably with the value of 10 from Kovasznay *et al.* (1970) although the higher Reynolds number for the present experiment must be considered partially responsible for the improvement. Some final evidence is shown in figure 18, which is a plot of S across the interface position at two points within the boundary layer. The function shows a sharp change in slope and enables a clear distinction to be made between the turbulent and the non-turbulent fluid.

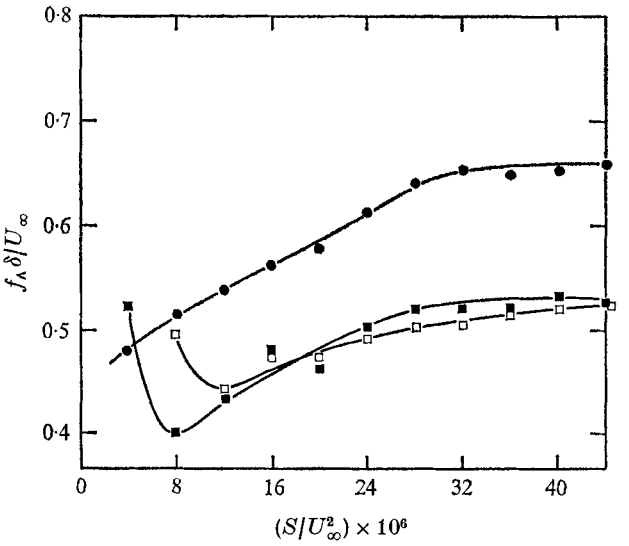

FIGURE 16. Influence of detector function upon crossing frequency. □, S and S_0; ■, S; ●, $(\partial u/\partial t)^2$.

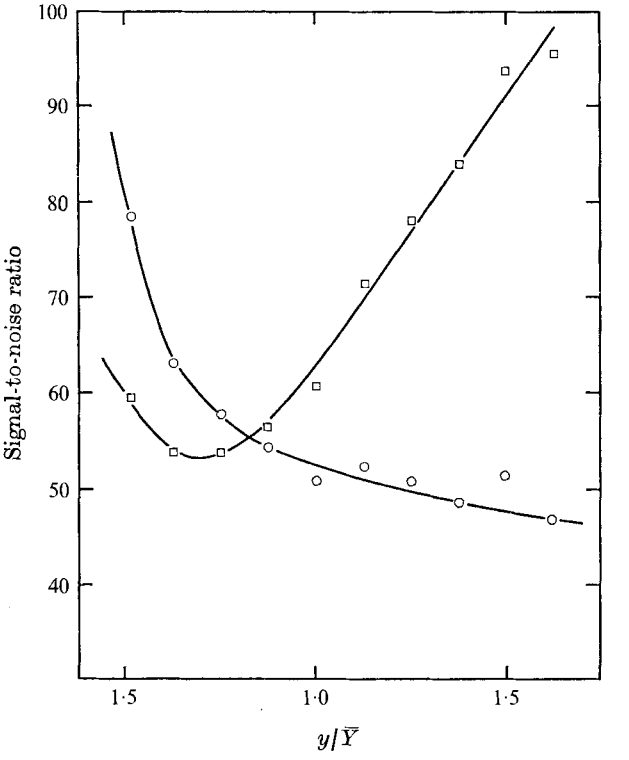

FIGURE 17. Turbulence criteria functions, signal-to-noise ratio. □, $\bar{\tilde{S}}/\tilde{\bar{S}}$; ○, $\bar{\tilde{S}}_0/\tilde{\bar{S}}_0$, $\bar{Y}$ is the value of y at which $\bar{I} = 0{\cdot}5$.

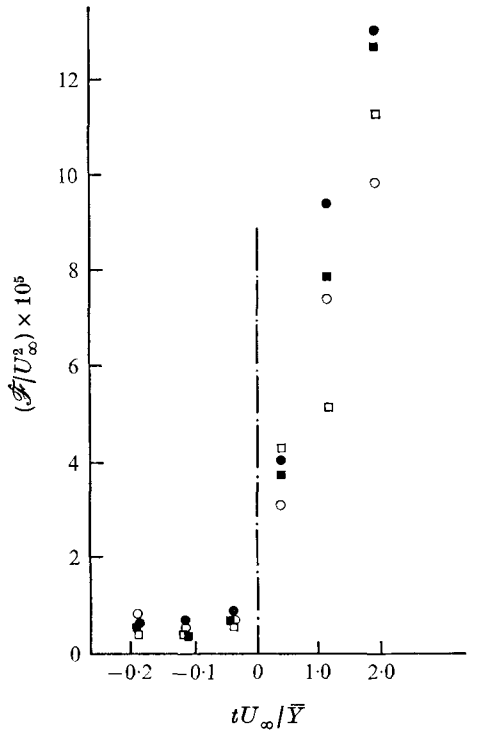

FIGURE 18. Variation of basic detector function $\mathscr{F} \equiv (\Delta u)^2 + (\Delta v)^2$ across turbulent interface. ○, upstream edge, $\bar{I} = 0{\cdot}51$; □, upstream edge, $\bar{I} = 0{\cdot}10$; ●, downstream edge, $\bar{I} = 0{\cdot}51$; ■, downstream edge, $\bar{I} = 0{\cdot}10$.

6. Discussion

It is clear that the underlying decisions behind any rationale or algorithm for deciding upon turbulence will remain open and that many options are possible. Bradshaw & Murlis (1973) have concluded that the best results are produced when no smoothing of the signal is used, the signal drop-out being eliminated by threshold levels applied to the signal and its derivative separately. We have in effect combined techniques, retaining the smoothing for both the signal and its derivative. Too long a hold time will obviously eliminate interesting, short-duration bursts from the signal and this is unacceptable. Spurious bursts, however, must be eliminated and in the absence of a perfect detector function, smoothing over a prechosen constant small period of time is a valid compromise which will not affect the legitimate burst statistics. We need only ensure that the window be no greater than the smallest scales of interest and this can be estimated from the known physics of the flow. It becomes clear though that such decisions will inevitably be influenced by the spatial scales of the fine structure. We note that, with the signal-plus-derivative technique which uses no smoothing, we are essentially viewing the flow through a window of variable width, conditioned directly by the frequency of the turbulent fluctuations. The minimum width of this window is effectively determined by the setting of the threshold level of the derivative signal. The result is a form of smoothing.

It was suggested by Kovasznay *et al.* (1970) that an iterative procedure could be used to define the threshold level, subsequent estimates being calculated as the square root of the product of r.m.s. values in the two fluid states. In attempting this in our present study it was found that convergence did not give physically realistic results, and we preferred instead to base the choice on the stability of a physical property (the length of the non-turbulent zone), which could be judged on other more readily measured dimensions, such as the nominal depth of the flow. Bradshaw & Murlis (1973), however, have noted that, when values of the criterion or detector functions are determined within the fully turbulent fluid, the procedure converges rather rapidly with any reasonable initial guess. The high signal-to-noise ratios in our present data (figure 17) indicate that we might expect similar results.

This research was sponsored by the National Research Council of Canada, Grant A-2746, and the Pulp and Paper Research Institute of Canada. The authors would like to express their appreciation to Peter Bradshaw for his informative comments on the manuscript.

REFERENCES

ANTONIA, R. A. 1972 *J. Fluid Mech.* **56**, 1.

ANTONIA, R. A. & BRADSHAW, P. 1971 *Imp. College Aero. Rep.* no. 71–04.

BRADSHAW, P. & MURLIS, J. 1973 *Imp. College Aero. Tech. Note*, no. 73–108.

CORRSIN, S. 1943 *N.A.C.A. Wartime Rep.* W-94.

CORRSIN, S. & KISTLER, A. L. 1955 *N.A.C.A. Rep.* no. 1244.

FIEDLER, H. E. & HEAD, H. R. 1966 *J. Fluid Mech.* **25**, 719.

GARTSHORE, I. S. 1966 *J. Fluid Mech.* **24**, 89.

HEDLEY, T. B. & KEFFER, J. F. 1974 *J. Fluid Mech.* **64**, 645.

HESKESTAD, G. 1965 *J. Appl. Mech.* **32**, 721.

KAPLAN, R. E. & LAUFER, J. 1968 *Proc. 12th Int. Cong. Appl. Mech., Stanford.*

KIBENS, V. & OSWALD, L. J. 1974 To appear.

KLEBANOFF, P. S. 1955 *N.A.C.A. Rep.*, no. 1247.

KOVASZNAY, L. S. G., KIBENS, V. & BLACKWELDER, R. F. 1970 *J. Fluid Mech.* **41**, 283.

KUO, A. Y. & CORRSIN, S. 1971 *J. Fluid Mech.* **50**, 285.

LUMLEY, J. L. & PANOFSKY, H. A. 1964 *The Structure of Atmospheric Turbulence.* Interscience.

OBOUKOV, A. M. 1962 *J. Fluid Mech.* **13**, 77.

PHILLIPS, O. M. 1972 *J. Fluid Mech.* **51**, 97.

SHEIH, C. M., TENNEKES, H. & LUMLEY, J. L. 1971 *Phys. Fluids*, **14**, 201.

SUNYACH, M. 1971 D.Sc. thesis, University of Lyon.

THOMAS, R. M. 1973 *J. Fluid Mech.* **57**, 549.

TOWNSEND, A. A. 1948 *Austr. J. Sci. Res.* **1**, 161.

TOWNSEND, A. A. 1949 *Austr. J. Sci. Res.* **2**, 451.

TOWNSEND, A. A. 1966 *J. Fluid Mech.* **26**, 689.

TOWNSEND, A. A. 1970 *J. Fluid Mech.* **41**, 13.

VAN ATTA, C. W. & CHEN, W. Y. 1970 *J. Fluid Mech.* **44**, 145.

WYGNANSKI, I. & FIEDLER, H. E. 1970 *J. Fluid Mech.* **41**, 327.